INL/RPT-24-80879-Revision-0

FFTF HT9 Cladding Microstructure Characterization

October 2024

Yachun Wang, Douglas L Porter, Liang Zhao, Bao-Phong Hoang Nguyen, Joshua Eddy Rittenhouse, Tanner Jason Mauseth, Tiankai Yao

Changing the World's Energy Future

Idaho National Laboratory

INL is a U.S. Department of Energy National Laboratory operated by Battelle Energy Alliance, LLC

INL/RPT-24-80879-Revision-0

FFTF HT9 Cladding Microstructure Characterization

Yachun Wang, Douglas L Porter, Liang Zhao, Bao-Phong Hoang Nguyen, Joshua Eddy Rittenhouse, Tanner Jason Mauseth, Tiankai Yao

October 2024

Idaho National Laboratory
Idaho Falls, Idaho 83415

http://www.inl.gov

Prepared for the
U.S. Department of Energy
Under DOE Idaho Operations Office
Contract DE-AC07-05ID14517

2024 Accomplishments Report Template

1. **Revision number (if applicable): N/A**
2. **Title: FFTF HT9 Cladding Microstructure Characterization**
3. **Principal Investigator: Yachun Wang**
4. **Team Members/ Collaborators: Douglas L. Porter, Liang Zhao, Bao-Phong H. Nguyen, Joshua E. Rittenhouse, Tiankai Yao, Tanner J. Mauseth**
5. **Introduction:**
   The sodium-cooled fast reactor (SFR) is a promising candidate for next generation nuclear reactors, operating at extreme conditions which include high temperatures (>500°C core outlet temperature) and significant neutron damage. High-Cr martensitic HT9 steel is an excellent candidate for SFR cladding and duct material due to its compatibility with liquid sodium, good thermal conductivity, resistance to void swelling, and strong creep rupture strength [1-4].However, the harsh in-core environment of SFRs can cause complex microstructural changes and mechanical property degradation in HT-9. Ensuring the safe use of HT9 cladding for metallic fuel requires both a thorough understanding of its mechanical response to microstructure evolution as well as reliable microstructure-sensitive modeling predictions. Microstructure-sensitive modeling of high temperature creep behavior in HT9 cladding for SFR applications currently lack experimental data to model the phenomena accurately. To fill this need, methods to perform microstructural characterization have been developed and performed on HT9.

6. **Project Description:**
   The development of microstructure-sensitive models to predict high temperature creep behavior in HT9 cladding requires a large, curated microstructure dataset of in-reactor irradiated HT9 cladding. Therefore, the primary objective of this work was to harvest HT9 cladding microstructure data by integrating state-of-the-art transmission electron microscopy (TEM)-based characterization techniques and deep learning (DL)-based methods for microstructure quantification analysis at Idaho National Laboratory (INL). Ten HT9 clad/U-10Zr samples extracted out of four FFTF (Fast Flux Test Facility) irradiated U-10Zr fuel pins (Table 1) were selected for this project. Microstructure features of interest were dislocations, precipitates, and martensitic boundaries. Dislocation quantification was emphasized in this work because dislocation microstructure and density are most prone to evolution upon neutron irradiation at elevated temperatures. Such evolution is directly linked to plastic deformation behavior and bulk mechanical properties in HT9 cladding. TEM can directly reveal dislocations at nanoscale; however, deriving accurate dislocation statistics remains a challenge. To overcome this challenge, this work developed a DL-based model to automatically detect and measure dislocation line microstructure in as-collected HT9 TEM micrographs. The model proved its high efficacy by accurately identifying dislocations in TEM micrographs containing high density dislocation networks (on the order of $10^{14} m^{-2}$). Additionally, this work established standardized procedures for data collection and data analysis to ensure consistency between datasets. The primary goal of this work was to benefit the nuclear material research community. Microstructural data obtained from this work will feed in microstructure-sensitive creep model development and validation led by Los Alamos National Laboratory (LANL). Overall, this effort is expected to improve high-temperature creep modeling of HT9 cladding in SFR environments, crucial for minimizing the risks of cladding failure and maximizing economic viability in the SFR energy sector.

Table 1. FFTF-irradiated HT9 cladding microstructure characterization matrix to support microstructure-sensitive HT9 creep model development. Red check mark indicates tasks completed in FY2024. The black cross symbol means to be completed in FY2025.

Fuel pin ID	Sample ID	Time averaged PICT (°C)	Neutron fluence (*10^22 n/cm^2)	Estimated dpa in the HT-9 cladding	Planned TEM lamella preparation using FIB OD=outer diameter ID=Inner diameter	TEM lamella preparation using FIB	TEM characterization microstructure	Data analysis
Fresh HT9	--	--	--	--	1	✓	✓	✓
195011 (MFF5) 92239 Heat	MNT86T	**556**	**14.24**	**63**	1 (OD) +1 (ID)	✓	✓	✓
	MNT87T	**612**	**11.97**	**53**	1 (OD) + 1 (ID)	✓	×	×
	MNT88T	**635**	**5.57**	**25**	1 (OD) + 1 (ID)	✓	✓	✓
193045 (MFF3) 92235 Heat	MNT83T	**615**	6.01	**26**	1 (OD) + 1 (ID)	✓	✓	✓
193114 (MFF3) 92235 Heat	MNT54C	**540**	**18.92**	**83**	1 (OD) + 1 (ID)	✓	×	×
	MNT46Z	**580**	**17.94**	**79**	1 (OD) + 1 (ID)	×	×	×
	MNT34Z	**630**	**9.12**	**40**	1 (OD) + 1 (ID)	×	×	×
193019 (MFF3) 92235 Heat	MNT62E	542	**17.98**	**79**	1 (OD)	×	×	×
	MNT63E	578	**15.11**	**67**	1 (OD) + 1 (ID)	×	×	×
	MNT64E	605	**7.68**	**34**	1 (OD) + 1 (ID)	×	×	×

7. **Accomplishments:**

Table 1 summarizes the microstructure characterization matrix for all selected samples. For the selected samples, the time-averaged peak inner cladding temperature (PICT) ranged from 540°C to 635°C. Estimated irradiation damage levels ranged from 25 to 83 dpa (displacement per atom). Work completed in FY2024 is highlighted with red check symbol. The entire work scope is planned to complete by FY2025. The accomplishment in FY2024 is summarized as follows: (1) dislocation microstructure characterization and quantification; (2) martensitic boundary characterization through 4DSTEM (four-dimensional scanning electron microscopy).

Dislocation microstructure characterization and quantification: Seven out of the eleven prepared TEM lamella (Table 1) were characterized using a Thermo Scientific Titan Themis scanning transmission electron microscope (STEM) at the Irradiated Material Characterization Laboratory (IMCL). Hundreds of STEM micrographs of dislocation microstructure were collected and required statistical dislocation analysis. To accelerate data analysis while attempting to prevent human bias in dislocation identification, this work developed an end-to-end deep learning-based method for automatic dislocation line detection and length measurement from TEM micrographs (Figure 1). By treating dislocations as edges rather than cracks or lines, two modules were designed to adapt the network from general edge detection to dislocation detection. Specifically, a rectification module was developed and integrated into the basic framework to enhance feature segmentation for continuous and non-cycle detection of TEM dislocations. Furthermore, a post-processing module was embedded into the framework to filter out redundant and overlapping dislocations. Following filtration, the method was trained using publicly accessible datasets [5, 6]. Finally, the trained method was used to automatically generate the location and length of dislocations for multiple in-house collected TEM micrographs (Figure 2a).

The full process of generating dislocation length results (Figure 2b) for each tested micrograph (Figure 2a) took only seconds, proving the method's high efficiency. Additionally, the generated dislocation length results showed high accuracy (>96%, Table 2) when compared to micrographs analysed manually by INL researchers (Figure 2c). Those results highlight the potential impact of the DL-based method developed in this work on saving human power and time for analysing labor-intense data. This method can be applied to large datasets of TEM micrographs containing high densities of dislocations (on the order of $10^{14}m^{-2}$). The manuscript highlighting the end-to-end deep learning-based method for dislocation analysis will be submitted in beginning of FY2025. By the end of FY2025, a large dataset of dislocation statistics for FFTF irradiated HT9 cladding will be generated, documented, and published.

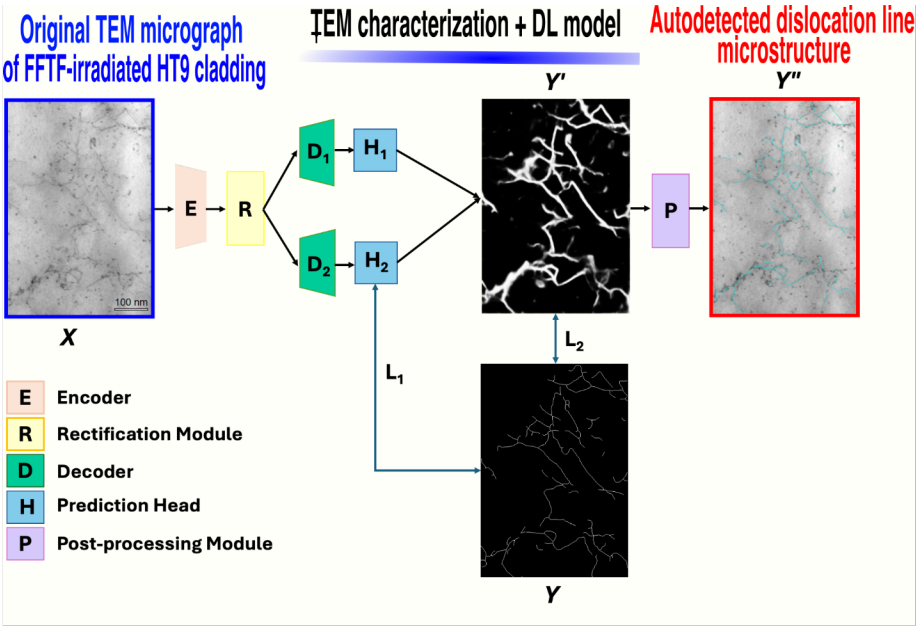

Figure 1. Overview of the deep learning (DL)-based model architecture for automatic detection and measurement of dislocation line microstructure in TEM micrographs. An input scanning TEM (STEM) micrograph X is fed into the encoder-decoder based framework. Two new modules, named rectification module and post-processing module, are designed and integrated into the framework for dislocation line detection and length quantification.

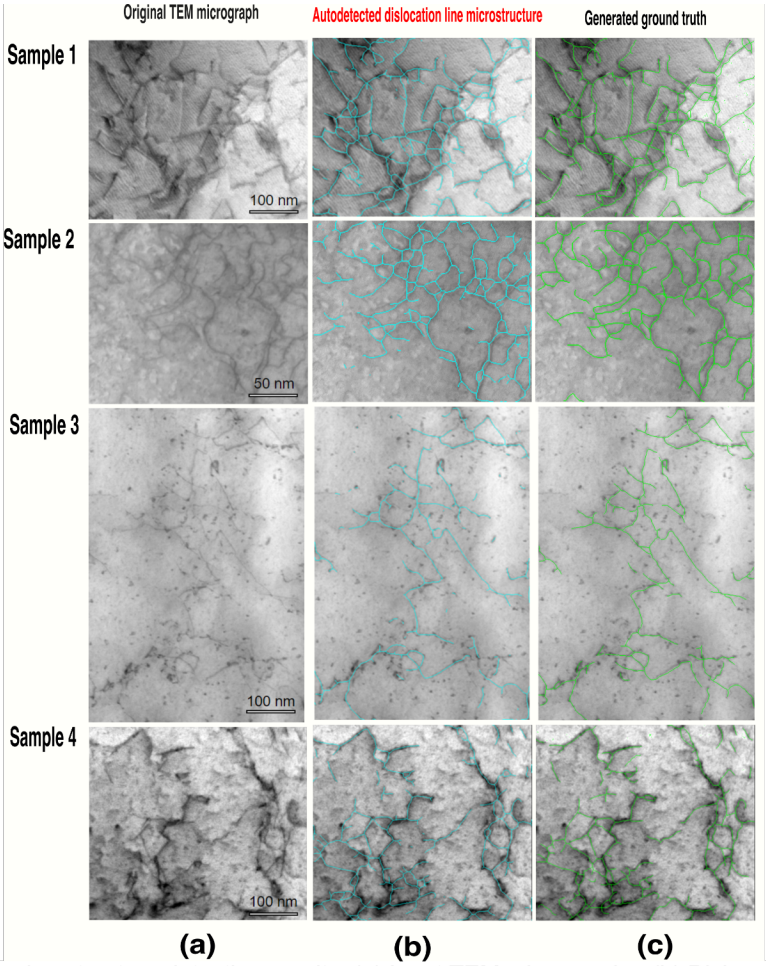

Figure 2. Dislocation microstructure detection results: (a) Input TEM micrographs; (b) Dislocation reconstruction (post-processing) of initially detected dislocation with rectification module; (c) Generated ground truth (GT) by manual labelling.

Table 2. DL-based method generated dislocation statistics for HT9 TEM micrographs showed in Figure 2(a). The accuracy (>96%) is calculated by dividing the DL-model generated results in Figure 2(b) with the ground truth (Figure 2c), demonstrating the high accuracy of the model to quantify high dislocation line density (on the order of 10^{14} /m^2).

Micrograph in Figure 2	Sample ID listed in Table 1	Micrograph dimension (pixel)		DL-model generated dislocation length (pixel)		Ground truth (GT) (pixel)	Accuracy (%)	Dislocation density (10^{14} /m^2)
		Height	Width	Figure 2(c)	Figure 2(d)			
1	MNT83T	326	399	4508	4959	4929	99.39	7.4028
2	MNT88T	231	280	2208	2884	2973	97.01	8.6580
3	Fresh HT9	653	450	3564	3642	3782	96.30	2.4066
4	Fresh HT9	458	513	4792	4870	4927	98.84	4.0248

Martensitic boundary characterization through 4DSTEM: In this work, 4DSTEM was applied to map phases and crystalline orientation as well as boundary characterization. Figure 3 shows preliminary 4DSTEM data for one of the MNT88T TEM lamella. The phase map in Figure 3b clearly revealed nanoscale $M_{23}C_6$ precipitates. Figure 3c shows the inverse pole figure (IPF) along with grain boundaries, where some preserved lath structure is clearly revealed. Figure 3c also reveals the onset of subgrain formation based on the subgrain boundaries (red lines). Comprehensive 4DSTEM data analysis will continue in FY2025.

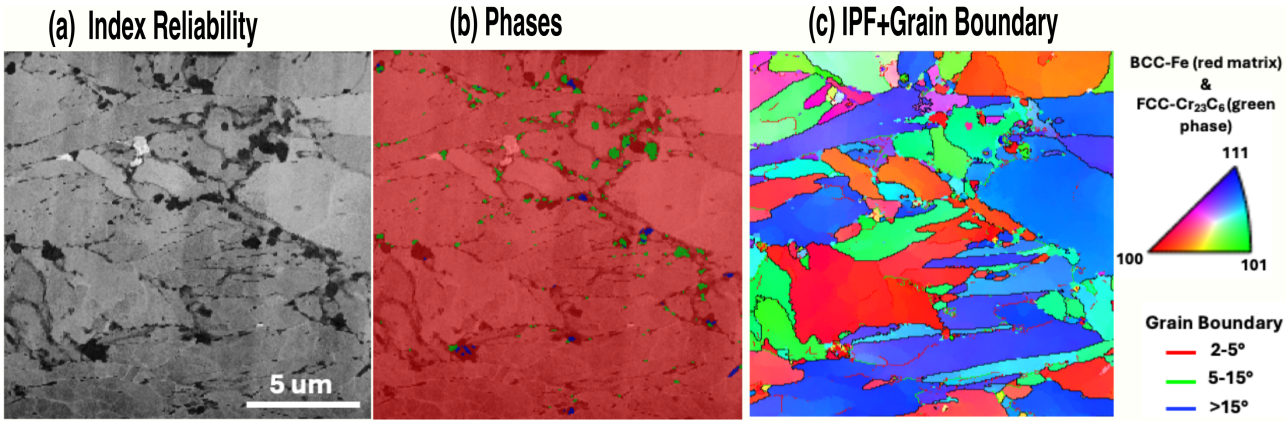

Figure 1. 4DSTEM characterization of phases, crystalline orientation, and martensitic boundary for a TEM lamella prepared for MNT88T sample listed in Table 1.

8. **Write one sentence on why this project is important.**
This work highlights a high-efficiency and accuracy, end-to-end deep learning-based method for automatic dislocation line detection and length measurement from TEM micrographs.

Yachun Wang_1: Caption Overview of the deep learning (DL)-based model architecture for automatic detection and measurement of dislocation line microstructure in transmission electron microscopy (TEM) micrographs. The input scanning TEM (STEM) micrograph X is fed into the encoder-decoder based framework. Two new modules, named rectification module and post-processing module, are designed and integrated into the framework for dislocation line detection and length quantification.

Yachun Wang _2: Caption Dislocation microstructure detection results: (a) Input TEM micrographs; (b) Dislocation reconstruction (post-processing) of initially detected dislocation with rectification module; (c) Generated ground truth (GT) by manual labelling.

Yachun Wang _3: Caption 4DSTEM characterization of phases, crystalline orientation, and martensitic boundary for a TEM lamella prepared for MNT88T sample listed in Table 1.

Reference

[1] R.L. Klueh, A.T. Nelson, Ferritic/martensitic steels for next-generation reactors, Journal of Nuclear Materials 371(1-3) (2007) 37-52.
[2] Y. Chen, Irradiation Effects of Ht-9 Martensitic Steel, Nuclear Engineering and Technology 45(3) (2013) 311-322.
[3] B.H. Sencer, J.R. Kennedy, J.I. Cole, S.A. Maloy, F.A. Garner, Microstructural stability of an HT-9 fuel assembly duct irradiated in FFTF, Journal of Nuclear Materials 414(2) (2011) 237-242.
[4] N. Hashimoto, R. Kasada, B. Raj, M. Vijayalakshmi, Radiation Effects in Ferritic Steels and Advanced Ferritic-Martensitic Steels, Comprehensive Nuclear Materials2020, pp. 226-254.
[5] D.A. Mély, J. Kim, M. McGill, Y. Guo, T. Serre, A systematic comparison between visual cues for boundary detection, Vision research 120 (2016) 93-107.
[6] P. Arbelaez, M. Maire, C. Fowlkes, J. Malik, Contour detection and hierarchical image segmentation, IEEE transactions on pattern analysis and machine intelligence 33(5) (2010) 898-916.